A Hall Sensor-Based Position Measurement Hybrid Magnetic Levitation System

Xing-Dong Fu[1], Guang-Zhong Cao[1*], Li-Jia Wang[1], Su-Dan Huang[1], Jian Zhou[2], and Xiao-Sheng Yang[1]

[1] Shenzhen University, Shenzhen, China.

[2] Xi'an Jiaotong University, Xi'an, China.

xingdongf@gmail.com, gzcao@szu.edu.cn, 1910294025@email.szu.edu.cn, hsdsudan@gmail.com, jzhou@mail.xjtu.edu.cn, yangxiaosheng27@gmail.com

Abstract

This paper presents a hall sensor-based position measurement of hybrid magnetic levitation system (MLS) developed in the laboratory for applications of contactless operations at a microscale. Cylindrical permanent magnets and iron-core electromagnetics are used to build a desire hybrid magnetic field of the MLS. The nonlinear magnetic flux density model of the MLS is first deduced. Based on the deduced model, the mathematical relation of the current supplied to the electromagnet and the position of the levitation object was obtained and analyzed. And then, the installation of the linear Hall-effect sensors was determined theoretically. Furthermore, the solution model for the position of the levitation unit was given. Finally, the effectiveness of the solution model of the MLS is validated by simulation analysis.

1 Introduction

As a typical application of magnetic actuators, magnetic levitation system (MLS) has been a popular research area in nowadays. MLS can be used in special environments and realize contactless operations due to the reason that there is no mechanical contact [1]. These environments which require contactless operations at a microscale include such as operating inside the human body [2]-[4], micro-manipulation robot in clean room [5] and bio-manipulation [6]. To achieve precise motion control of the MLS, the optical-based devices, such as laser sensors or camera are generally used to measure the position of the levitated object [11],[12], however, there is an obvious limitation for the operation in a nontransparent environment. In [13], a methodology to determine the position of a magnetically guided robot in horizontal planes using Hall-effect sensors is proposed. The Hall-effect

sensors solve the above limitation and it is inspirational to this paper. From [13], using hall sensors to obtain the position information of MLS is an effective and significant method.

The MLS presented in this paper has the features of simple structure, low power consumption, low cost and complex magnetic fields. To give a more complete account of the research work, this paper is organized as follows. Section II describes the structure and the magnetic mode of the MLS. Section III discuss the laying position of linear Hall-effect sensors and the solution model for the position of the levitation unit was proposed. Base on the finite element simulation data, section IV shows the results of the proposed model. Conclusion of this paper is given in Section V.

2 System Description

2.1 The Structure of the Magnetic Levitation System

The MLS presented in this paper is shown in Fig. 1. The system consists of a magnetic drive unit (MDU), a levitated object with a solid cylindrical permanent magnetic, and a DSP control system. The MDU has twelve hollow cylindrical permanent magnetics and four iron-core electromagnets. The hollow permanent magnetic array of the MDU can form a permanent magnetic field (see Fig. 2) which provides part of the levitation force applied on the levitated object. Therefor the permanent magnetic array plays a key role of reducing the energy consumption of the MDU. The bottom plate which made of printed circuit board (PCB) in Fig. 2 is used to mount the sensors and the electromagnets. The four electromagnets are used to form a desired magnetic field to regulate the position of the levitated object. The linear Hall-effect sensors are installed in the center of the bottom plate to measure the two-dimensional horizontal motion of the levitated object. The DSP controller acts as a central processing unit to first calculate the position of the levitated object based on position feedback from the linear Hall-effect sensors, and second to output current to drive the electromagnets. Finally, a personal computer is used to communicate with the DSP controller base on UART and monitor the levitation system.

2.2 The Magnetic Model of the Magnetic Levitation System

In this paper, the magnetic field of the MDL is produced by four iron-core electromagnets, twelve hollow cylindrical permanent magnets and one solid cylindrical permanent magnet. On account of the magnetic field superposition principle, the analysis of the magnetic field can be simplified to a problem that to analyze the magnet field of a solid cylindrical permanent magnet and an iron-core electromagnet. Using the current model, the magnetic field produced by a solid cylindrical permanent magnet at a random point P (x, y, z) in free space is:

$$\begin{cases} B_x = M\dfrac{\mu_0}{4\pi}\displaystyle\int_0^h\int_0^{2\pi} \dfrac{R\cos\theta_0(z-z_0)}{((x-R\cos\theta_0)^2+(y-R\sin\theta_0)^2+(z-z_0)^2)^{3/2}}d\theta_0 dz_0 \\ B_y = M\dfrac{\mu_0}{4\pi}\displaystyle\int_0^h\int_0^{2\pi} \dfrac{R\sin\theta_0(z-z_0)}{((x-R\cos\theta_0)^2+(y-R\sin\theta_0)^2+(z-z_0)^2)^{3/2}}d\theta_0 dz_0 \\ B_z = M\dfrac{\mu_0}{4\pi}\displaystyle\int_0^h\int_0^{2\pi} \dfrac{-R(\sin\theta_0(y-R\sin\theta_0)+\cos\theta_0(x-R\cos\theta_0))}{((x-R\cos\theta_0)^2+(y-R\sin\theta_0)^2+(z-z_0)^2)^{3/2}}d\theta_0 dz_0 \end{cases} \tag{1}$$

where B_x, B_y, and B_z are the x-, y- and z-component magnetic flux density of the solid cylindrical permanent magnet at point P (x, y, z), R, M and h are the radius, the magnetization and the height of the permanent magnet, μ_0 is the permeability of vacuum. In order to simplify the following expression,

as the laying position of the cylindrical permanent magnet is given, (1) can be rewritten as a function of R:

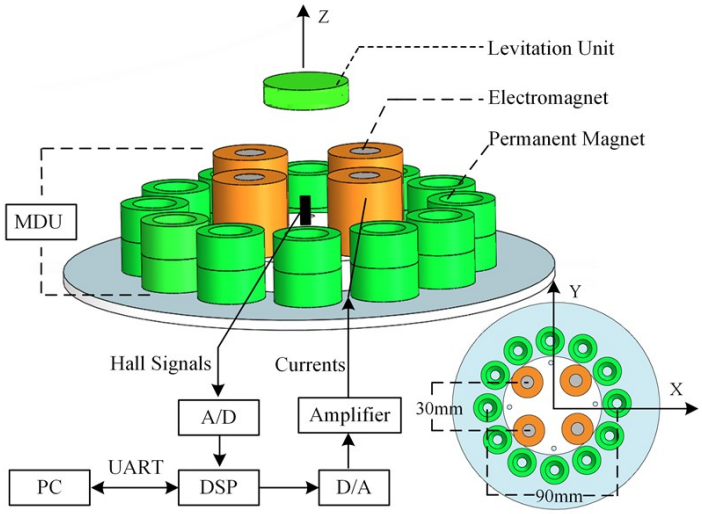

Figure 1: Structure of the magnetic levitation system

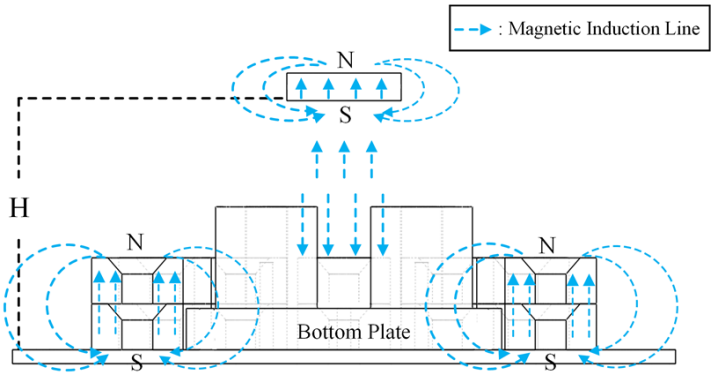

Figure 2: The magnetic field diagram of the MLS with currents applied to the electromagnets were all zero

$$\begin{cases} B_x = f_1 x_{pm}(R,x,y,z) \\ B_y = f_1 y_{pm}(R,x,y,z) \\ B_z = f_1 z_{pm}(R,x,y,z) \end{cases} \tag{2}$$

Base on (2), the magnetic field produced by a hollow cylindrical permanent magnet use in the MDU is:

$$\begin{cases} B_x = f_1 x_{pm}(R_{out} - R_{in},x,y,z) \\ B_y = f_1 y_{pm}(R_{out} - R_{in},x,y,z) \\ B_z = f_1 z_{pm}(R_{out} - R_{in},x,y,z) \end{cases} \tag{3}$$

where R_{out} and R_{in} are the outside radius and inside radius of the hollow cylindrical permanent magnet. Here, the magnetic model of the permanent magnetics in the MLS is defined. And then the magnetic field produced by a single iron-core electromagnet at point $P\ (x, y, z)$ is [11]:

$$\begin{cases} B_x = \beta \dfrac{\mu_0 \sigma I}{4\pi} \displaystyle\int_{r_{in}}^{r_{out}} \int_0^L \int_0^{2\pi} \frac{R\cos\varphi(z-h)}{((x-R\cos\varphi)^2+(y-R\sin\varphi)^2+(z-h)^2)^{3/2}} d\varphi dh dR \\ B_y = \beta \dfrac{\mu_0 \sigma I}{4\pi} \displaystyle\int_{r_{in}}^{r_{out}} \int_0^L \int_0^{2\pi} \frac{R\sin\varphi(z-h)}{((x-R\cos\varphi)^2+(y-R\sin\varphi)^2+(z-h)^2)^{3/2}} d\varphi dh dR \\ B_z = -\beta \dfrac{\mu_0 \sigma I}{4\pi} \displaystyle\int_{r_{in}}^{r_{out}} \int_0^L \int_0^{2\pi} \frac{\cos\varphi(x-R\cos\varphi)+\sin\varphi(y-R\sin\varphi)}{((x-R\cos\varphi)^2+(y-R\sin\varphi)^2+(z-h)^2)^{3/2}} d\varphi dh dR \end{cases} \tag{4}$$

where β is the magnetic flux density factor of the iron-core effect in enhancement of the magnetic field, and σ is the winding density of the electromagnet. Its unit is turns per unit area, I is the current supplied to the electromagnet, r_{in} and r_{out} are the inner and outer radius of the electromagnet, respectively, and is the length of each coil.

Base on the above discussions, the magnetic model of the MLS is given by (2), (3) and (4). How to use the model and the hall sensors to determine the position of the levitation unit will be described in the next.

3 Hall Sensor-Based Position Measurement

3.1 Installation of the Linear Hall-effect Sensors

There are three magnetic field sources in the MLS, a solid cylindrical permanent is the levitated unit, the permanent magnets and the electromagnets are used in the MDU. In fact, when the Hall-effect sensors were installed in the magnetic drive unit, only the position of the levitated object change and current supply to the electromagnets change cause the magnetic field measured by the linear Hall-effect sensors change. Therefore, the key to the installation of the linear Hall-effect sensors is to find a position where will not be affected by the electromagnet's magnetic field, so that the position of the levitated object can be obtained from the change of the magnetic field measured by the linear Hall-effect sensors.

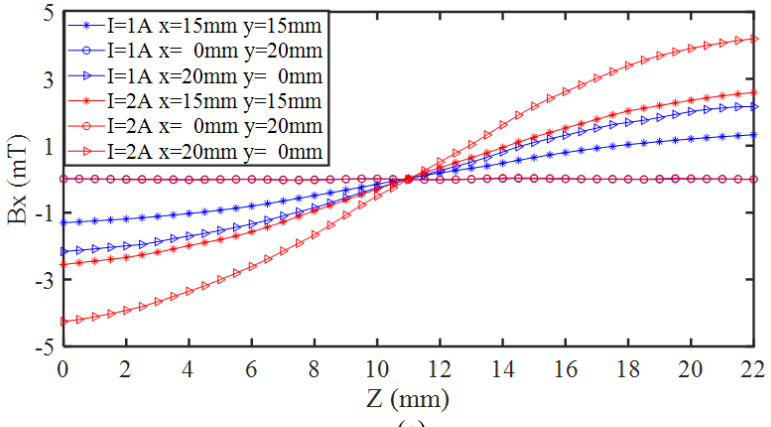

(a)

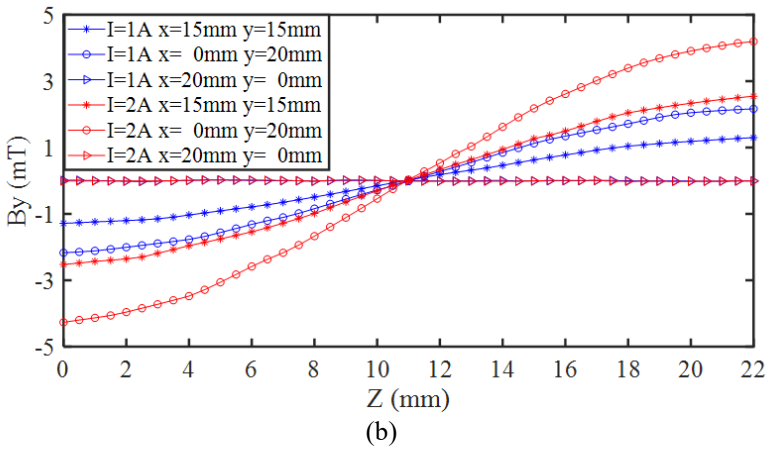

(b)

Figure 3: The horizontal component of the electromagnet's magnetic flux density under different current and different horizontal position versus z-axis. (a) x-component. (b) y-component

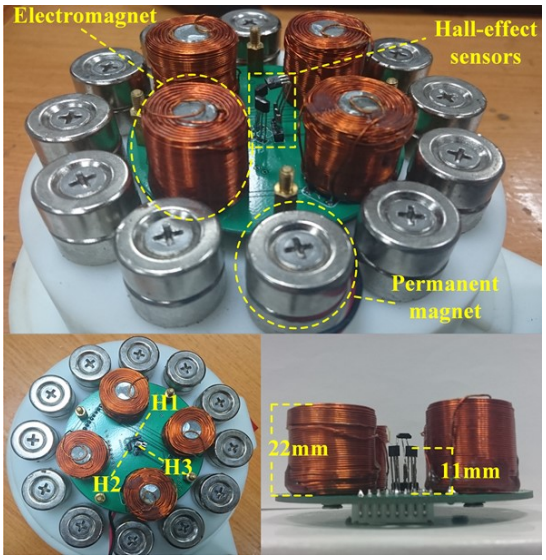

Figure 4: The laying position of the Hall sensors in the experimental device

To find the laying position of the linear Hall-effect sensors, using (4) to explore the magnetic field distribution of an electromagnetic. The electromagnet used in the calculation model has the following geometric parameters: N = 500 turns, r_{out} =10.5 mm, r_{in} = 4.5 mm, and L = 22 mm. Fig.3 shows that no matter how the current applied to the electromagnet change, the horizontal components of the magnetic field at a height of L/2 are always zero. The laying position of the linear Hall-effect sensors is determined (see Fig.4) base on this characteristic of the electromagnet. Hall sensor H1 and H2 are used to measure the magnetic flux density in horizontal direction, H3 is used to the measure the magnetic flux density in vertical direction, by the way.

3.2 Solution Model for the Position of Levitation unit

According to the installation of the hall sensors, the interference of electromagnets to the sensors can be ignored. On the other hand, due to the fact that the magnetic field generated by the permanent

magnet in MDU is a static magnetic field, the measured values of hall sensors only change with the position of the levitation unit. In fact, the nonlinear relationship between the position of the levitation unit and the measured value of the hall sensors satisfies formula (1). However, due to the complexity of formula (1), it is difficult to obtain the position of the levitation unit directly from the magnetic flux density information. Therefore, a solution model for the position of levitation unit based on B-P(Back-Propagation) neural network is designed and it process structure is shown in Fig.5.

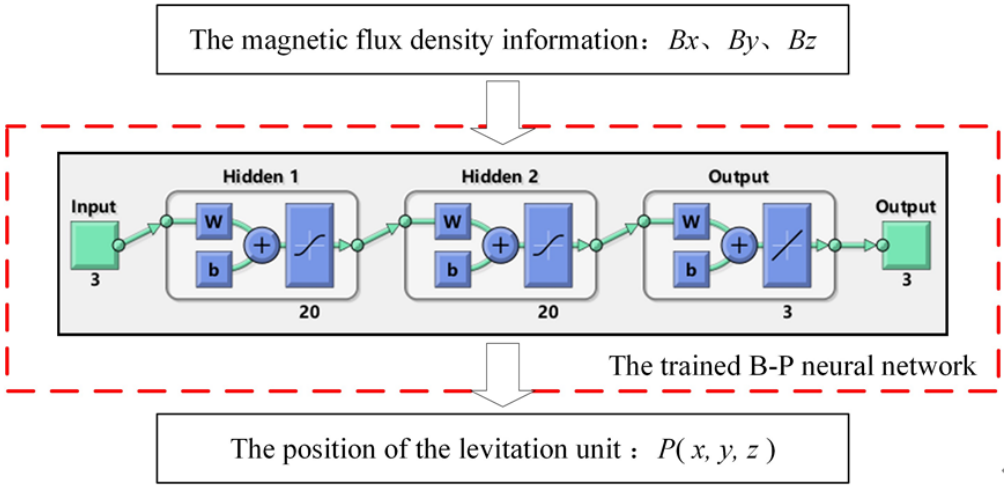

Figure 5: The process structure of the proposed model

The training data (B_x, B_y, B_z, x, y, z) of the network come from the finite element model (FEM) via ANSYS Maxwell software. The value range of FEM is -60mm< x <60mm, -60mm< y <60mm, 37mm< z <47mm. Fig.6(a), Fig.2(b) and Fig.2(c) show the magnetic field of the HMLS at z=37mm, I=0A.

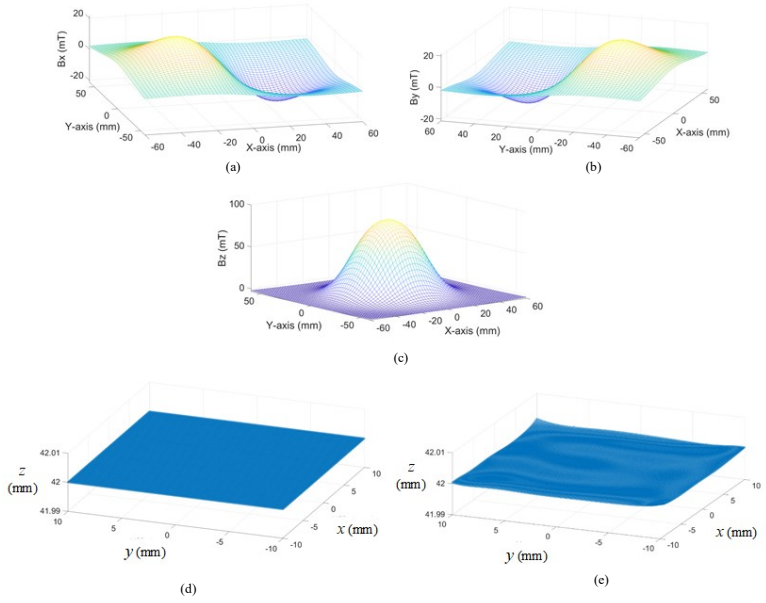

Figure 6: The simulation results

Significance	Symbol	Value	Unit
Intensity of magnetization	M	8900	kA/m
The inner diameter of a cylindrical hollow permanent magnet	R_{in}	2	mm
The outer diameter of a cylindrical hollow permanent magnet	R_{out}	5	mm
The height of a cylindrical hollow permanent magnet	h	20	mm
The inner diameter of the electromagnetic coil	r_{in}	4.5	mm
The outer diameter of the electromagnetic coil coi	r_{out}	10.5	mm
The current in the electromagnetic coil	I	1	
The number of turns of the electromagnetic coil	N	500	Am
The length of the electromagnetic coil	L	22	mm

Table 1: Parameters of hybrid repulsive magnetic levitation system

4 Simulation Results and Analysis

The proposed position measurement of the HMLS is validated by FEM analysis and the error caused by the noise in sampling circuit is ignored in the simulation. Parameters of the HLMS is listed in Table 1.

Fig.6 (d) shows the position of the sampling point for the magnetic flux density of the levitation unit. By analyzing the sampled data, Fig.6 (e) shows the results of the proposed solution model. According to the simulation results in Fig.6 (d) and Fig.6 (e), the solution position approaches to the desired position, where the maximum absolute errors of x-axis, y-axis and z-axis are 1.3×10-3mm, 1.2×10^{-3}mm and 1.3×10^{-3}mm, respectively. The maximum relative errors are 0.0065%, 0.0065% and 0.0180%, respectively. The effectiveness of the proposed method is verified.

5 Conclusion

In this paper, the analytical nonlinear modelling and the installation of the linear Hall-effect sensors were presented for the MLS developed in the laboratory, which is to show the potential application in the contactless operation for the magnetic levitation system. The results of the finite elements analysis verified the effectiveness of the nonlinear modelling of the MLS. Experimental device is developed based on the analytical nonlinear modelling. The future work will be focused on the effective control method of the developed MLS by employing the linear Hall-effect sensors to detect the position based on the analytical nonlinear model

References

[1] S. Yim, K. Goyal, and M. Sitti, “Magnetically actuated soft capsule with the multimodal drug release function,” IEEE/ASME Trans. Mechatronics, vol. 18, no. 4, pp. 1413–1418, Aug. 2013

[2] F. Munoz, G. Alici, W. Li and M. Sitti, “Size Optimization of a Magnetic System for Drug Delivery With Capsule Robots,” in IEEE Transactions on Magnetics, vol. 52, no. 5, pp. 1-11, May 2016.

[3] Y. Zhang, M. Chi and Z. Su, “Critical Coupling Magnetic Moment of a Petal-Shaped Capsule Robot,” in IEEE Transactions on Magnetics, vol. 52, no. 1, pp. 1-9, Jan. 2016.

[4] Y. Zhang et al., “Design, analysis and experiments of a spatial universal rotating magnetic field system for capsule robot,” 2012 IEEE International Conference on Mechatronics and Automation, Chengdu, 2012, pp. 998-1003.

[5] K. Park, K. Ahn, S. Kim, and Y. Kwak, “Wafer distribution system for a clean room using a novel magnetic suspension technique,” IEEE/ASME Trans. Mechatronics, vol. 3, no. 1, pp. 73–78, Mar. 1998.

[6] S. Martel, J.-B. Mathieu, O. Felfoul, A. Chanu, E. Aboussouan, S. Tamaz, P. Pouponneau, L. Yahia, G. Beaudoin, G. Soulez, and M. Mankiewicz, “Automatic navigation of an untethered device in the artery of a living animal using a conventional clinical magnetic resonance imaging system,” Appl. Phys. Lett., vol. 90, art. no. 114105, 2007.

[7] A. M. Benomair, A. R. Firdaus and M. O. Tokhi, “Fuzzy sliding control with non-linear observer for magnetic levitation systems,” 2016 24th Mediterranean Conference on Control and Automation (MED), Athens, 2016, pp. 256-261.

[8] H. R. Karampoorian and R. Mohseni, “Control of a nonlinear magnetic levitation system by using constraint generalized model predictive control,” ICCAS 2010, Gyeonggi-do, 2010, pp. 48-51.

[9] H. Chiang, C. Fang, W. Lin and G. Chen, “Second-order sliding mode control for a magnetic levitation system,” 2011 8th Asian Control Conference (ASCC), Kaohsiung, 2011, pp. 602-607.

[10] J. Yang, Y. Lee and O. Kwon, “Development of magnetic force modeling equipment for magnetic levitation system,” ICCAS 2010, Gyeonggi-do, 2010, pp. 29-33.

[11] E. Shameli, “Design, implementation and control of a magnetic levitation device,” Ph.D. dissertation, Dept. Mech. Eng., University of Waterloo, Waterloo, ON, Canada, 2008.

[12] P. Mane, P. Dugwekar and A. Ingole, “Position control of magnetic levitation system,” 2015 International Conference on Industrial Instrumentation and Control (ICIC), Pune, 2015, pp. 1626-1629.

[13] X. Zhang, M. Mehrtash and M. B. Khamesee, “Dual-Axial Motion Control of a Magnetic Levitation System Using Hall-Effect Sensors,” in IEEE/ASME Transactions on Mechatronics, vol. 21, no. 2, pp. 1129-1139, April 2016.